Silicon Nanodisks via a Chemical Route

Wen-Jing Qin,[†] Xiao-Bo Yang,[†] Ying-Wei Lu,[†] Jing Sun,[†] Sergei A. Kulinich,[‡] and Xi-Wen Du*,[†]

School of Materials Science and Engineering, Tianjin University, Tianjin, 300072, P. R. China, and Department of Applied Sciences, University of Quebec, Saguenay, PQ, Canada G7H 2B1

Received January 6, 2008. Revised Manuscript Received March 26, 2008

Silicon nanodisks were synthesized by combining phase separation of SiO with extreme conditions created by the pulsed-laser-ablation-in-liquid technique. Their structure and growth mechanism are carefully investigated in this study. The disk shape is found to result from the restrained growth along the [110] direction due to the absorption of SiO_2 phase on the {110} planes, which have the highest surface energy. Such silicon nanodisks give blue light emission and thus may have potential applications in nanoelectronics.

Introduction

Physical properties of nanostructures are well-known to be closely related to their size and shape. For example, the luminescence of CdSe nanorods was reported to be strongly affected by their shape,[1,2] and Cu nanorods exhibited anisotropic optical properties related to their aspect ratio.[3] Silicon nanomaterials are expected to possess potentially useful electrical, optical, mechanical, and chemical properties,[4] and therefore many efforts have been made to obtain various Si nanostructures, such as nanodots,[5] nanowires,[6] nanotubes,[7] and multilayered configurations.[8]

Silicon nanodots, as a system with three-dimensional confinement, were shown to demonstrate a strong quantum confinement and give intensive luminescence in the visible range, which is significantly different from the bulk material.[9] Silicon nanowires, being a system with two-dimensional confinement whose surface can be easily modified, were demonstrated to possess unique characteristics required for ultrasensitive, miniaturized molecular sensing applications.[10] They are also recommended as a good candidate for investigating the dependence of electrical and thermal transport or mechanical properties on dimensionality and size reduction.[11] One more two-dimensional system, Si nanotubes, has been recently synthesized as a novel material.[7] Since such nanotubes have the same structure as carbon nanotubes, similar electrical properties may be expected.[12]

As a less common nanostructure, nanodisks have been prepared in several material systems, e.g., Ag,[13] Co,[14] and ZnO,[15] demonstrating many attractive properties.[16] Recently, Kubota and co-workers have fabricated Si nanodisks through a top-down approach of neutral-beam etching of single-crystal Si.[17,18] The nanodisks obtained showed single-electron-charging effect and are expected to have great potential for the development of quantum-effect devices.[17,18] Compared with the top-down approach, chemical synthesis, one of the bottom-up routes, has several advantages, such as simplicity, lower costs, and higher productivity. However, chemical synthesis of Si nanodisks has not been reported thus far.

In the present work, we propose a chemical route to synthesize silicon nanodisks by combining phase separation of SiO with the pulsed-laser-ablation-in-liquid (PLAL) technique. The phase separation of SiO precursor has been widely employed to prepare Si nanowires and nanodots in previous works.[19,20] On the other hand, PLAL is a cold-wall process where pulsed laser can provide extreme conditions, such as high temperature, high pressure, and high cooling rates.[21–23] Therefore, chemical reactions under PLAL

* Corresponding author. E-mail: xwdu@tju.edu.cn.
[†] Tianjin University Tianjin.
[‡] University of Quebec.

(1) Hu, J.; Li, L.; Wang, W.; Manna, L.; Wang, L.; Alivisatos, A. P. *Science* **2001**, *292*, 2060.
(2) Lisiecki, I.; Pileni, M. P. *J. Am. Chem. Soc.* **1993**, *115*, 3887.
(3) Ding, Z. F.; Quinn, B. M.; Haram, S. K.; Pell, L. E.; Korgel, B. A.; Bard, A. J. *Science* **2002**, *296*, 1293.
(4) Liu, A. S.; Jones, R.; Liao, L.; Rubio, D. S.; Rubin, D.; Cohen, O.; Nicolaescu, R.; Paniccia, M. *Nature* **2004**, *427*, 615.
(5) Pavesi, L.; Dal Negro, L.; Mazzoleni, C.; Franzo, G.; Priolo, F. *Nature* **2000**, *408*, 440.
(6) Cui, Y.; Lieber, C. M. *Science* **2001**, *291*, 851.
(7) Chen, Y. W.; Tang, Y. H.; Pei, L. Z.; Guo, C. *Adv. Mater.* **2005**, *17*, 564.
(8) Garcia-Santamaria, F.; Ibisate, M.; Rodriguez, I.; Meseguer, F.; Lopez, C. *Adv. Mater.* **2003**, *15*, 788.
(9) Canham, L. T. *Appl. Phys. Lett.* **1990**, *57*, 1046.
(10) Shao, M. W.; Shan, Y. Y.; Wong, N. B.; Lee, S. T. *Adv. Funct. Mater.* **2005**, *15*, 1478.
(11) Au, F. C. K.; Wong, K. W.; Tang, Y. H.; Zhang; Y. F.; Bello, I.; Lee, S. T. *Appl. Phys. Lett.* **1999**, *75*, 1700.
(12) Yang, X. B.; Ni, J. *Phys. Rev. B* **2005**, *72*, 195426.
(13) Maillard, M.; Giorgio, S.; Pileni, M. P. *Adv. Mater.* **2002**, *14*, 1084.
(14) Puntes, V. F.; Krishnan, K. M.; Alivisatos, A. P. *Science* **2001**, *291*, 2115.
(15) Xu, C. X.; Sun, X. W.; Dong, Z. L.; Yu, M. B. *Appl. Phys. Lett.* **2004**, *85*, 3878.
(16) Kim, C.; Kim, Y. J.; Jang, E. S.; Yi, G. C.; Kim, H. H. *Appl. Phys. Lett.* **2006**, *88*, 093104.
(17) Kubota, T.; Hashimoto, T.; Ishikawa, Y.; Samukawa, S.; Miura, A.; Uraoka, Y.; Fuyuki, T.; Takeguchi, M.; Nishioka, K.; Yamashita, I. *Appl. Phys. Lett.* **2006**, *89*, 233127.
(18) Kubota, T.; Hashimoto, T.; Takeguchi, M.; Nishioka, K.; Uraoka, Y.; Fuyuki, T.; Yamashita, I.; Samukawa, S. *J. Appl. Phys.* **2007**, *101*, 124301.
(19) Zhang, R. Q.; Zhao, M. W.; Lee, S. T. *Phys. Rev. Lett.* **2004**, *93*, 095503.
(20) Wang, N.; Tang, Y. H.; Zhang, Y. F.; Lee, C. S.; Lee, S. T. *Phys. Rev. B* **1998**, *58*, R16024.
(21) Yang, G. W. *Prog. Mater. Sci.* **2007**, *52*, 648.

10.1021/cm800037f CCC: $40.75
Published on Web 05/17/2008

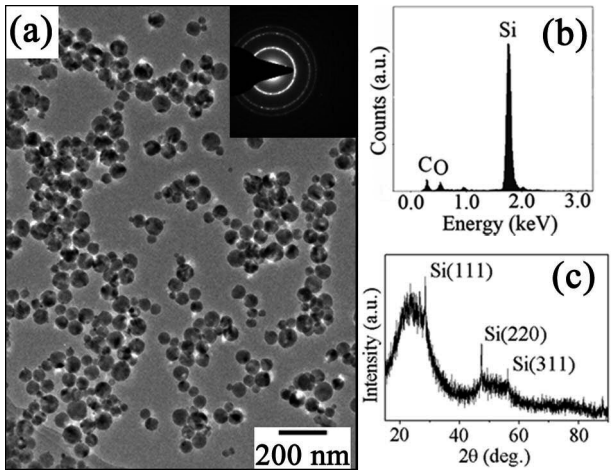

Figure 1. (a) Overview of HF-etched Si nanostructures (sample A), the inset showing a typical SAED pattern. (b) EDS spectrum. (c) XRD pattern.

conditions often lead to unique products. On the basis of the above considerations, we combined the phase separation of SiO powder with the extreme conditions created by the PLAL technique, which resulted in a large number of silicon nanodisks being fabricated. Visible light emission was detected from the product, which implies potential applications of such nanodisks in optical and electronic devices.

Experimental Procedures

Commercial SiO powder from Beijing Xmengtai Inc. (purity 99.99%, 200 mesh) was used as a starting material. A Nd:YAG pulsed laser was employed to irradiate a SiO suspension (0.2 g in 3 mL of deionized water) in a glass cuvette for 120 min at room temperature. The wavelength, frequency, and pulse width were 1064 nm, 20 Hz, and 1.2 ms, respectively. The laser beam with a single pulse energy of 4.895 J was focused ~5 mm below the liquid surface with a spot size of 0.2 mm. The as-prepared suspension (hereafter labeled as sample A) was of dark-yellow color. For comparison, sample B had its irradiation time reduced to 10 min and sample C was prepared with a single pulse energy of 28.025 J, all the other parameters being the same as for sample A. For the convenience of further observations, the products were first filtered, to separate remaining SiO, and then etched with HF solution (35.35 wt %, 1 mL) for 12 h to remove surface SiO_2. The morphology and structure were determined in a FEI Technai G^2 F20 transmission electron microscope (TEM) equipped with a field emission gun. The composition was analyzed with an Oxford INCA energy-dispersive X-ray spectroscopy (EDS) module attached to the TEM. The phase structure was investigated by using a Rigaku D/max 2500v/pc X-ray diffractometer (XRD). Photoluminescence (PL) measurements were performed at room temperature using a Hitachi F-4500 fluorescence spectrometer with excitation by monochromatic light of 5.9 eV from a Xe lamp.

Results and Discussion

Figure 1a shows a low-magnification TEM image of HF-etched sample A. The product consists of a large number of nanocrystals (NCs) with apparently round shape. The EDS spectrum in Figure 1b shows that the NCs mainly contain Si with a small amount of oxygen. The XRD pattern (Figure 1c) of the sample matches well with the data of diamond-like silicon (JCPDS PDF card No. 27−1402), with the peaks being indexed as (111), (220), and (311). The broad bands arise from a glass holder used to support the sample powder. At the same time, the selected-area-electron-diffraction (SAED) pattern shown as the inset in Figure 1a proves the nanostructures are crystalline. The squares of radii of the diffraction rings correlate as 3:8:11:16:19 very precisely, also supporting the diamond structure of the NCs.

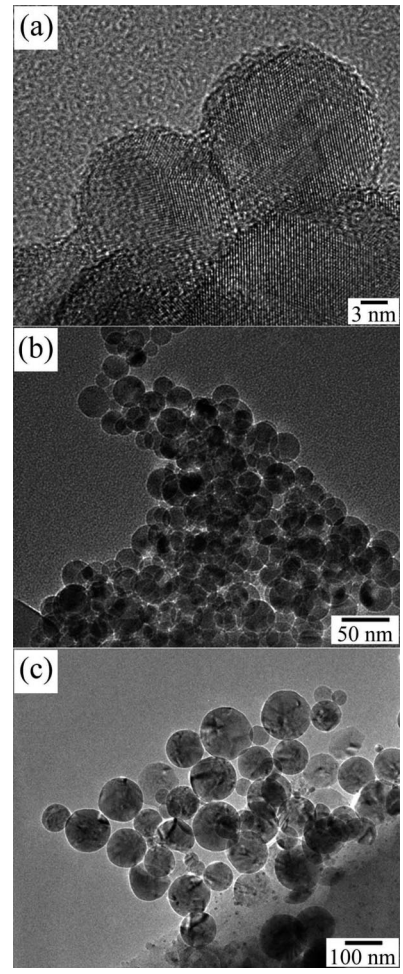

Figure 2. Typical TEM images of Si nanostructures from sample A. The diameter of the nanostructures is about (a) 10 nm, (b) 20 nm, and (c) 100 nm.

Figure 2 shows aggregates of the NCs with different size observed in sample A, the latter normally varying from 10 to 400 nm. The NCs with similar size were found to band together, forming aggregates. Interestingly, the contrast in TEM images was observed to be homogeneous across all the NCs analyzed (see e.g. Figure 2c), irrespective of their diameter. This suggests a disk shape for all the nanostructures synthesized.

To verify the disk shape of the NCs in sample A, three approaches were used. First, a two-dimensional TEM image was transformed into three-dimensional one based on the contrast difference in the initial image. As a result, disk-shaped structures are clearly seen in Figure 3a. Second, a NC in the edge-on state was found in a TEM image, as

(22) Hodak, J. H.; Henglein, A.; Giersig, M.; Hartland, G. V. *J. Phys. Chem. B* **2000**, *104*, 11708.
(23) Du, X. W.; Qin, W. J.; Lu, Y. W.; Han, X. ; Fu, Y. S.; Hu, S. L. *J. Appl. Phys.* **2007**, *102*, 013518.

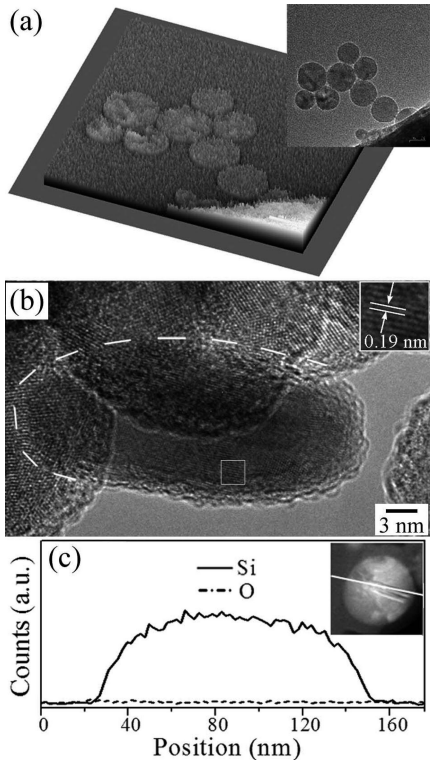

Figure 3. (a) Three-dimensional image of Si nanostructures (sample A) converted from the TEM image shown in the inset. (b) HRTEM image of a NC in edge-on state, where the dotted line marks the NC boundaries and the inset shows an enlarged image of the area in the frame. (c) Elemental linescan across a nanocrystal. The inset shows a scanning transmission electron microscopy image with the linescan track.

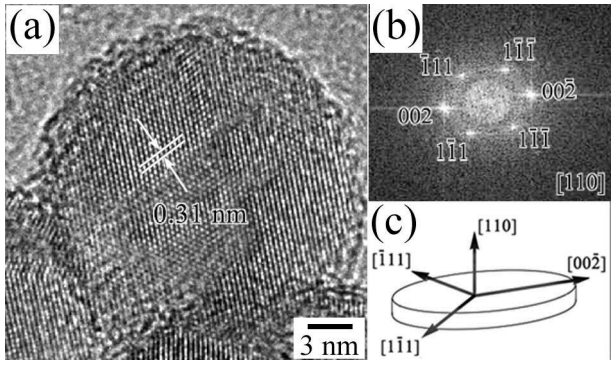

Figure 4. (a) Typical HRTEM image of Si nanodisk from sample A. (b) FFT pattern derived from the image in part a. (c) Schematic diagram of the crystal structure of the nanodisk.

shown in Figure 3b. The nanoparticle does not show the round shape, looking rather rectangular, which agrees well with the side view of a nanodisk. The interplanar distance of the atomic planes parallel to the disk faces is 0.19 nm (Figure 3b, inset), coinciding with the spacing of the (110) atomic planes. Third, elemental linescan was conducted to confirm the shape and composition of the particles. As can be seen in Figure 3c, the Si concentration across the particle is nearly constant, which proves the particle is disk-like rather than spherical. All the above results demonstrate that the nanoparticles possess a relatively unusual disk shape.

Figure 4a shows an HRTEM image of a nanodisk as it is viewed along the normal to its faces. The interplanar distance of 0.31 nm can be easily found, which corresponds to the (111) spacing of Si with the diamond structure. As shown

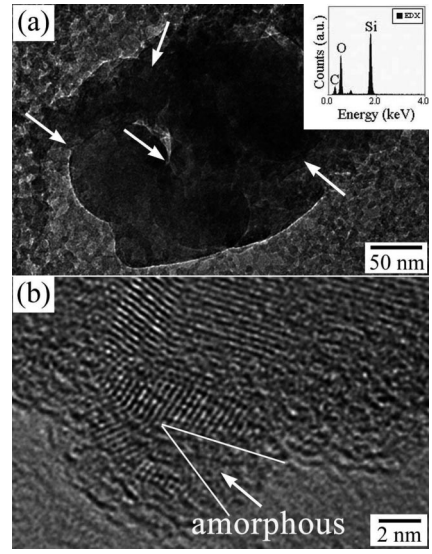

Figure 5. (a) Typical TEM image of nonetched product with several nanodisks marked with arrows. (b) HRTEM image of the structure at the edge of a Si nanodisk, where an amorphous area between an attached Si cluster and a nanodisk is pointed out with an arrow and the area boundaries are shown with white lines.

in Figure 4b, the fast Fourier transform (FFT) analysis of the nanodisk gives a [110] oriented diffraction pattern, which indicates that the [110] axis of Si is normal to the faces of the disk observed. The crystallographic directions of the nanodisk are schematically shown in Figure 4c, where the upper and lower disk faces are the (110) planes and possible planes at the lateral surface are expected to be (111), (002), and others perpendicular to the (110) plane.

To investigate the growth mechanism of the nanodisks, we also performed TEM analysis of an as-prepared sample without HF acid etching. It can be seen in Figure 5a that in such a product the disks are embedded in an amorphous matrix. The EDS spectrum taken over the amorphous area reveals a high concentration of oxygen (Figure 5a, inset). In Figure 5b, a Si cluster is seen which appears to be separated from the nanodisk by an oxide layer. This allows us to make conclusions on the latest growth stage of the nanodisks being studied.

On the basis of the above results, we propose the following mechanism for the nanodisk formation. SiO particles are first vaporized under the pulsed-laser irradiation, after which the converted SiO gas subsequently separates into Si and SiO_2 (Figure 6a). Si atoms tend to aggregate as a crystalline core, while SiO_2 species are excluded outward to decrease the total system energy. Among the crystallographic facets of Si, the {110} planes have the highest surface energy of 1.43 J m^{-2} (see Table 1). They are also known to possess the superior capability of absorbing SiO_2 species. Therefore, SiO_2 clusters are expected to preferably deposit on the {110} planes and assemble into compact SiO_2 layers. As a result, the growth of the silicon core along the [110] direction becomes restrained (Figure 6b). Such restraint in one dimension growth gives rise to the formation of nanodisks, with diameter increasing until the lateral surface is fully blocked with SiO_2 (Figure 6c). Any further phase separation can only generate clusters attaching on the surface of nanodisks, as shown in Figure 5b.

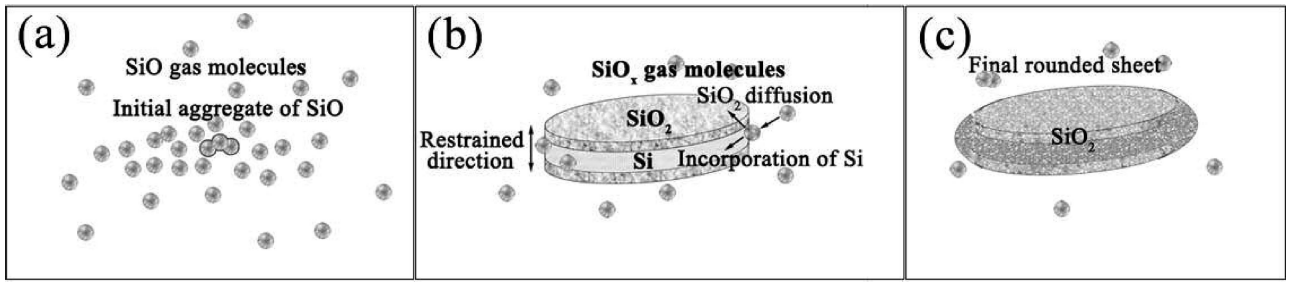

Figure 6. Schematic illustration of the Si nanodisk growth mechanism: (a) SiO gas is evaporized from SiO powder, (b) SiO_2 species attach on (110) facets of the silicon core, and (c) nanodisk formation caused by the restrained growth.

Table 1. Surface Energy of Various Facets of Silicon Crystal

facet	surface energy ($J \cdot m^{-2}$) experiment[24]	theory[25]
(111)	1.23	1.405
(100)	1.36	1.488
(311)	1.38	1.48
(110)	1.43	1.721

The influence of the experiment duration and powder density of laser pulses on the product structure and size was also investigated, the results being presented in Figure 7. As the irradiation time was reduced to 10 min, the disk size in sample B was found to vary mainly from 30 to 40 nm, with the largest NC size being below 100 nm. This size is more homogeneous and smaller than that in sample A, implying that nanodisks may grow intermittently under different laser pulses. Consequently, long-time irradiation leads to larger nanodisks. On the other hand, as a higher pulse energy of 28.025 J was employed, the product in sample C appears to be porous spheres of mixed Si nanocrystallites and amorphous silica (labeled with 1 in Figure 7b). During TEM observation, some spheres collapsed under the electron irradiation (e.g., the sphere labeled with 2), after which Si crystallites and silica could be observed clearly (see Figure 7b, inset). This finding suggests the decomposition of SiO under the higher pulse energy was so rapid that its phase separation, controlled by atomic diffusion, could not proceed sufficiently to form Si nanodisks. It also lends support to the formation mechanism of the Si nanodisks via phase separation.

The PL spectra recorded from both as-prepared and aged (60 days) suspension are presented in Figure 8a. The as-prepared sample shows a broad PL band ranging from 2.0 to 4.0 eV with the apex at 2.8 eV. After 60 days, the peak position does not change markedly, whereas the PL intensity slightly increases. The direct photographs illustrate that the as-prepared sample gives blue emission under the irradiation from a 254 nm UV lamp (Figure 8b, right). Since the nanodisks are relatively large to exhibit quantum confinement, the observed blue emission is believed to be from oxide-related defects on their surface. However, the luminescent mechanism still needs further investigations.

Conclusions

We synthesized silicon nanodisks by combining phase separation of SiO with extreme conditions created by the PLAL technique. The disk shape is believed to be the result of the restrained growth along the [110] direction due to the absorption of SiO_2 species on the (110) planes with the highest surface energy. The nanodisks gave blue light

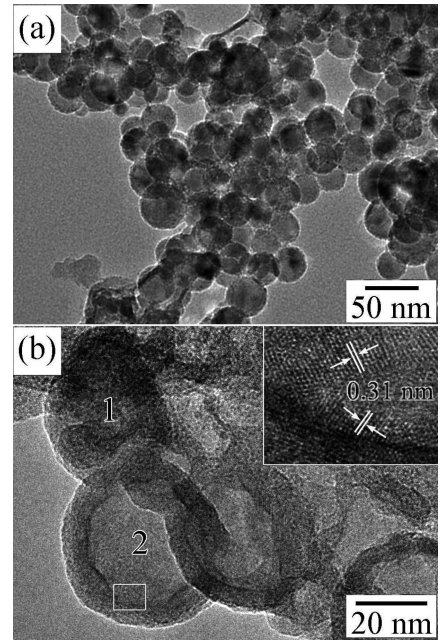

Figure 7. TEM images of HF-etched samples B (a) and C (b) obtained for shorter irradiation time (B) and by using a higher single pulse energy (C). Spheres 1 and 2 show typical morphologies before and after electron irradiation, respectively. Inset is the HRTEM image of the area in the frame.

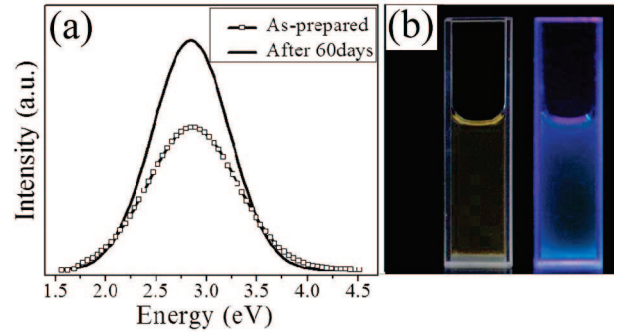

Figure 8. (a) PL spectra of as-prepared and aged for 60 days suspension of Si nanodisks from sample A under 5.9 eV excitation. (b) Direct photographs of as-prepared sample A taken under natural light (left) and 254 nm UV lamp (right).

(24) Eaglesham, D. J.; White, A. E.; Feldman, L. C.; Moriya, N.; Jacobson, D. C. *Phys. Rev. Lett.* **1993**, *70*, 1643.

(25) Gilmer, G. H.; Bakker, A. F. *Mater. Res. Soc. Symp. Proc.* **1991**, *209*, 135.

emission under ultraviolet irradiation, which can be ascribed to oxide-related defects on their surface. The approach of phase separation combined with the PLAL technique looks promising for preparing novel nanostructures and thus can be extended to other material systems.

Acknowledgment. This work was financially supported by the Natural Science Foundation of China (Nos. 50402010 and 50672065) and the Program for New Century Excellent Talents in University.

CM800037F